Journal of Mountain Area Research
Vol. 9, 2024
https://doi.org/10.53874/jmar.v9i0.206

*Full length article*

# OCCURRENCES OF SOLID INCLUSIONS OF SILICATE AND BASE METAL SULFIDE MINERALS IN CHROMITITE OF KHANOZAI OPHIOLITE, PAKISTAN: EVIDENCE FROM MELT EVALUATIONS

*Muhammad Ayoub Khan, Razzaq Abdul Manan, Muhammad Panezai, Abdullah*

Centre of Excellence in Mineralogy, University of Balochistan, Quetta, Pakistan

**ABSTRACT**

Chromitite bodies occur in the wide mantle portion of Khanozai ophiolite. This peridotite is largely composed of harzburgite, dunite and minor lherzolite. Chromitite occurs in Khanozai ophiolite mainly in massive, disseminated, banded and nodular forms. The Khanozai chromitites contains a variety of silicate and BMS mineral inclusions. They include anhydrous silicates like olivine, clinopyroxene, hydrous silicate inclusions of amphibole, and BMS mineral inclusions such as millerite, chalcopyrite, stibnite, and occasional pyrite and linnaeite. The silicate mineral inclusions occur as monomineralic as well as polymineralic phases. The shapes of these inclusions tend to follow the growth plane of host chromite. Textures and forms of these inclusions reveal that some inclusions were trapped during magmatic stage, whereas many inclusions were trapped during recrystallization of chromite. BMS inclusions are millerite, chalcopyrite, and stibnite. They occur isolated inclusions and at some places associated with silicate mineral inclusions. It is suggested that these BMS inclusions were generated due to the separation of sulfide-bearing liquid from silicate magma.

**KEYWORDS**: Silicate, base metal sulfide, inclusions, chromite, Khanozai Ophiolite

*Corresponding author Email: Ayoub.cemuob@gmail.com

## 1. INTRODUCTION

Chromitite in ophiolitic peridotite occurs in the forms of pods, lenses, and nodules. The composition of podiform chromite mainly dependent on the nature of melt and degree of partial melting of the mantle (1-2). For instance, parental magma of high-Cr and high-Al chromitite are boninitic and MORB like tholeiitic melts, respectively (3-7). Chromitite contains various inclusions of silicate and sulfide minerals. Zhob valley ophiolitic belt is an extended belt stretches from Zhob town to Quetta city around 300 km in western Pakistan which indicates a suture between Indian and Afghan Plates. The Zhob valley ophiolitic belt contains three ophiolitic bodies like Khanozai, Muslim Bagh and Zhob ophiolites. Thick mantle sections in these ophiolites host large chromitite deposits. Amon these ophiolitic bodies, Khanozai Ophiolite comprises a thick mantle section. Mantle section or peridotite composed largely of highly serpentinized harzburgite, dunite and minor lherzolite 8). The peridotite of Khanozai ophiolites hosts large chromitite bodies which occur in the forms of pods and lenses. The thickness of pods is up to 4 m while chromitite lenses reaches up to 25 cm (9). Highly serpentinized dunite envelopes enclose these chromitite bodies. Massive to semi-massive, disseminated, nodular, and layered or banded forms are common in these chromitites. This study represents the mineral and composition of silicate, and base metal sulfide (BMS) inclusions found in chromitite of Khanozai Ophiolite.

## 2. GEOLOGICAL SETTING

Boundary of Indian and Eurasian Plates is marked by Indus Suture Zone (ISZ). northwestern tectonic contact of Indian plate is demarcated by ophiolitic chain with the southeastern part of Afghan block. In these collisional zones between with Afghan block contains numerous mafic-ultramafic (ophiolitic) complex (10, 11). The ophiolitic bodies occur in a linear fashion in Pakistan which are divided into (i) the northern ophiolitic belt, and (ii) the western ophiolitic belt. Northen ophiolitic chain includes the Shangla–Mingora ophiolite, the Jijal complex, the Chilas complex, the Sapat complex, the Dargai (Skhakot–Qila) complex, and the Dras ophiolites or igneous complexes whereas western belt Mélange unit is mixture of volcanic and volcaniclastic rocks associated with pelagic
A thick mantle section is dominantly composed of serpentinized harzburgite with altered dunite and minor mylonitized/banded lherzolite (8).

contains Bela, Khanozai, Muslim Bagh, Zhob and Waziristan ophiolites. Khanozai Ophiolite is the part of Zhob valley ophiolites which is located near Khanozai town (Fig.1). Calcareous belt, suture belt and flysch belt form the surrounding area of this ophiolite. Loralai Formation (Jurassic) and Wulgai Formation (Triassic) of Calcareous belt occur immediately underlying the Khanozai Ophiolite. These formations are composed of abundant limestones, shales, and lesser amounts of sandstones, marls, and occasional conglomerates (13). The by the Suture belt consist of Zhob valley ophiolites including Khanozai Ophiolite overlying calcareous belt (14; Fig.1). In the north of Suture belt, Flysch belt is exposed (Fig.1) and makes non-conformity with ophiolite. The belt comprises of Nisai Formation (Eocene–Oligocene) limestone, shale, marl that grades to Khojak Formation (Oligocene) composed of shale and sandstone, and the Khojak Formation progressively gives way to the younger fluvial and lacustrine sedimentary successions (15). Khanozai Ophiolite Complex contains all ophiolitic units like crustal and mantle portions, metamorphic sole rocks, and underlying mélange. The crustal section is mainly composed of mafic-ultramafic cumulates which comprises of dunite and pyroxenite and both foliated as well as layered gabbros (16).

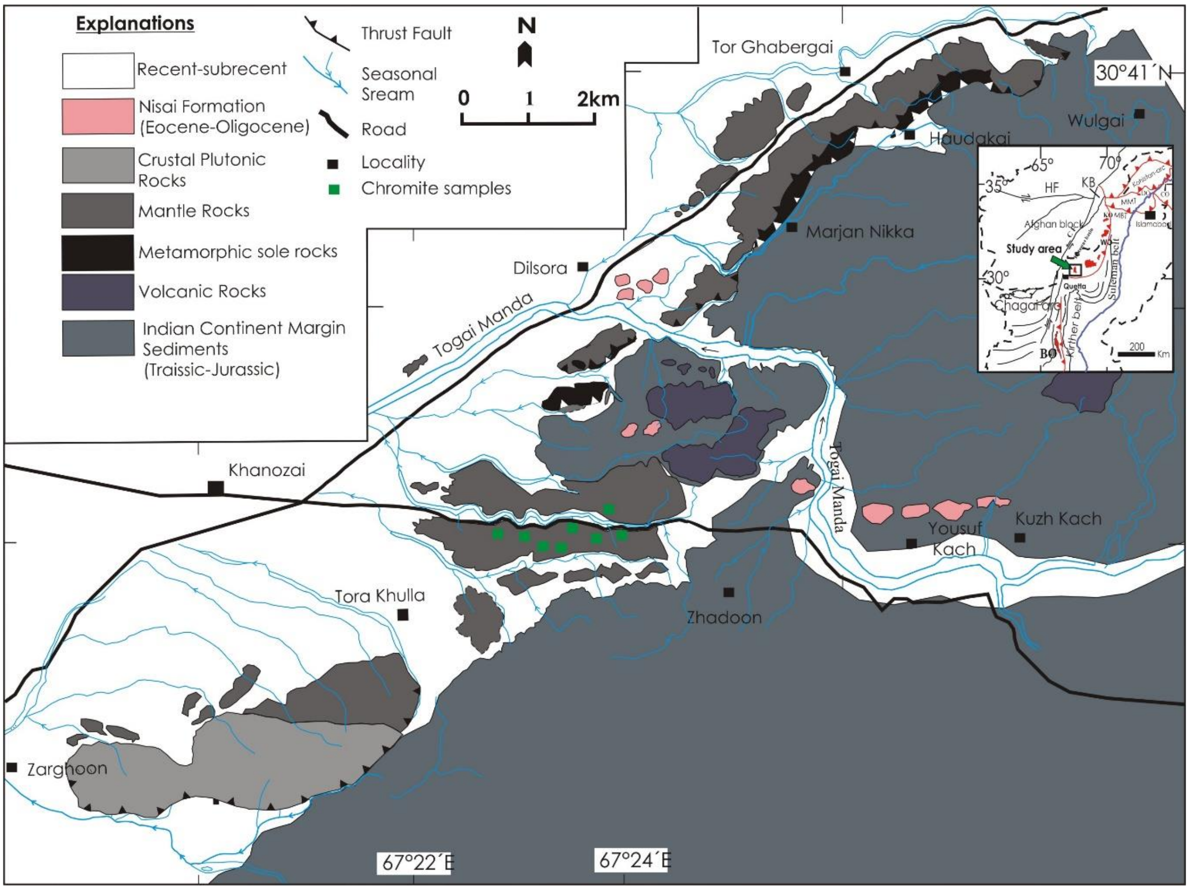


**Figure 1**. Geological map of Khanozai Ophiolite showing the outcrops of mantle, crustal, volcanic and metamorphic rocks of Khanozai Ophiolite and chromite sample locations (modified after Ulhaq et al., 2019 and Ali et al., 2019).

## 3. FIELD FEATURES

The mantle peridotite covers a large part of the Khanozai Ophiolite. This peridotite contains ultramafic tectonite (also named as foliated peridotite) as well transition zone dunite. Peridotite contains mainly harzburgite with subordinate dunite and lherzolite which are highly serpentinized. The lower part of the mantle section is mylonitized and shows banded structures (Fig.2a). Harzburgite and dunite are interlayered at some place and make banded structure (Fig.2b). Transition zone dunite makes hill which mainly composed of dunite (Fig.2c). Chromitite in Khanozai Ophiolite largely occur as pods of several meters in size. These pods are mainly formed from massive, semi-massive, disseminated with little banded and nodular chromitites (Fig-2d-f).

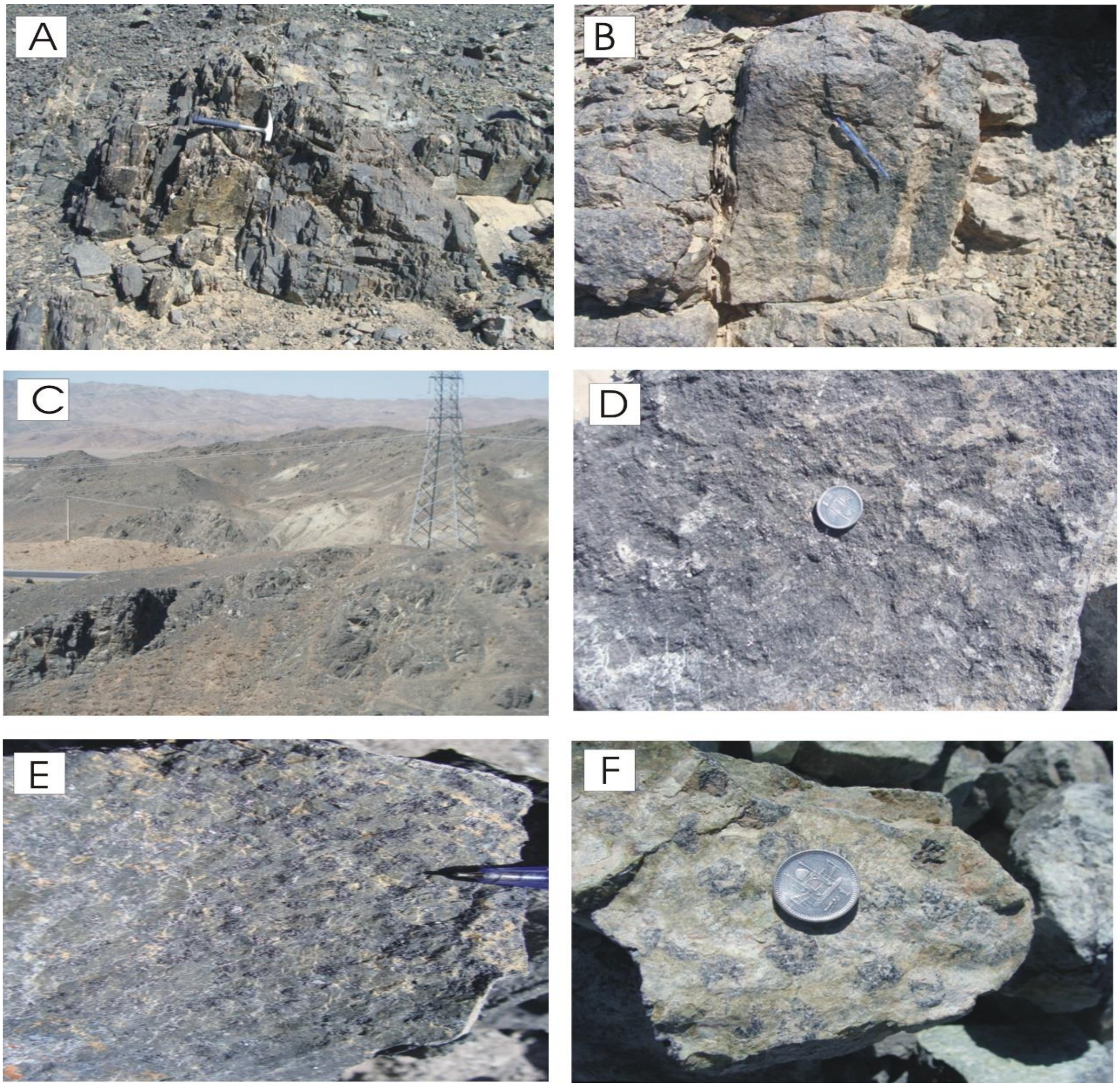


**Figure 2.** Field photographs show (**a**) Banded lherzolite in basal peridotite (**b**) bands of harzburgite and dunite (**c**) Small hills of dunite (**d**) massive chromitite (**e**) disseminated chromitite (**f**) nodular chromitite.

## 4. PETROGRAPHY

The mantle section of Khanozai ophiolite covers about 60% of the total area covered by the Khanozai Ophiolite Complex (Fig. 1). The mantle section contains dominantly highly serpentinized harzburgite, dunite and minor lherzolite found in the lower portion of peridotite.

### 4.1. Lherzolite

Lherzolite is composed of olivine, orthopyroxene, and clinopyroxene with a minor number of Cr-Spinel grains. Serpentine is found as secondary mineral. Lherzolite shows mainly porphyritic, porpyroclastic and mylonitic texture. At some places, phenocryst of clinopyroxene, medium to large grains, are enclosed by olivine and Cr-spinel, while occasionally, stretched grains of pyroxene and olivine are also found. Further, exsolution lamellae and twinning are common in clinopyroxene (Fig.3a).

### 4.2. Dunite

The dunite rock contains largely highly serpentinized olivine with minor orthopyroxene. Dunite exhibits interlocking and mesh texture in which the unaltered or partially altered cores of olivine grains are surrounded by serpentine (Fig.3b). Olivine makes subhedral to anhedral shapes and is fine to medium in size. Olivine is largely altered to serpentine while few grains are partially altered and mostly show island cores surround by the network of serpentine and Cr-spinel. A small faction of orthopyroxene is found as phenocryst within the matrix of altered olivine grains. The shape of orthopyroxene grains is subhedral to anhedral. Some opaque grains are found in the factures or interstices of olivine grains.

### 4.3. Harzburgite

Olivine, orthopyroxene and minor clinopyroxene and Cr-spinel are the principal constituents of harzburgite rock (Fig. 3c). The olivine is partially to completely altered to serpentine in harzburgite. The alteration of olivine to serpentine reaches up to 60%. Orthopyroxene occurs as a phenocryst as well as main constituent mineral. The most obvious texture identified in harzburgite rock is porphyritic texture. This texture is formed due to orthopyroxene phenocrysts enclosed in the groundmass of olivine, orthopyroxene and minor clinopyroxene. The grains of orthopyroxene and clinopyroxene are largely subhedral in shapes that make hypidiomorphic and granular textures.

### 4.4. Chromitite

Chromitite deposits found in the mantle peridotite Khanozai ophiolite in forms of lenses, pods, banded and nodular structures. Pods reach up to 4 m in thickness while lenses of chromitite are found up to 25 cm. The studied chromitites from Khanozai ophiolite are massive–semi massive, disseminated, banded, and nodular in texture. Optically, magmatic texture is common in Khanozai chromitites exhibit whereas some chromitite grains are brecciated and deformed. Chromitites of massive are medium to coarse-grained, largely subhedral in shape and some interlocking grains of chromite showing orthocumlate textures (Fig. 3d). Single chromite grains show cumulate textures. In this texture very thin veins and interstices in the chromite grains are filled by serpentine (Fig.3e). Some massive chromitites show brecciation and pull-apart textures (Fig.3f). Disseminated form of chromitites are largely subhedral and less commonly euhedral in shape (Fig.3g). The investigated chromites of all forms are largely fresh whereas few grains display typical Ferrit-chromite alteration along cracks and boundaries (Fig.3h).

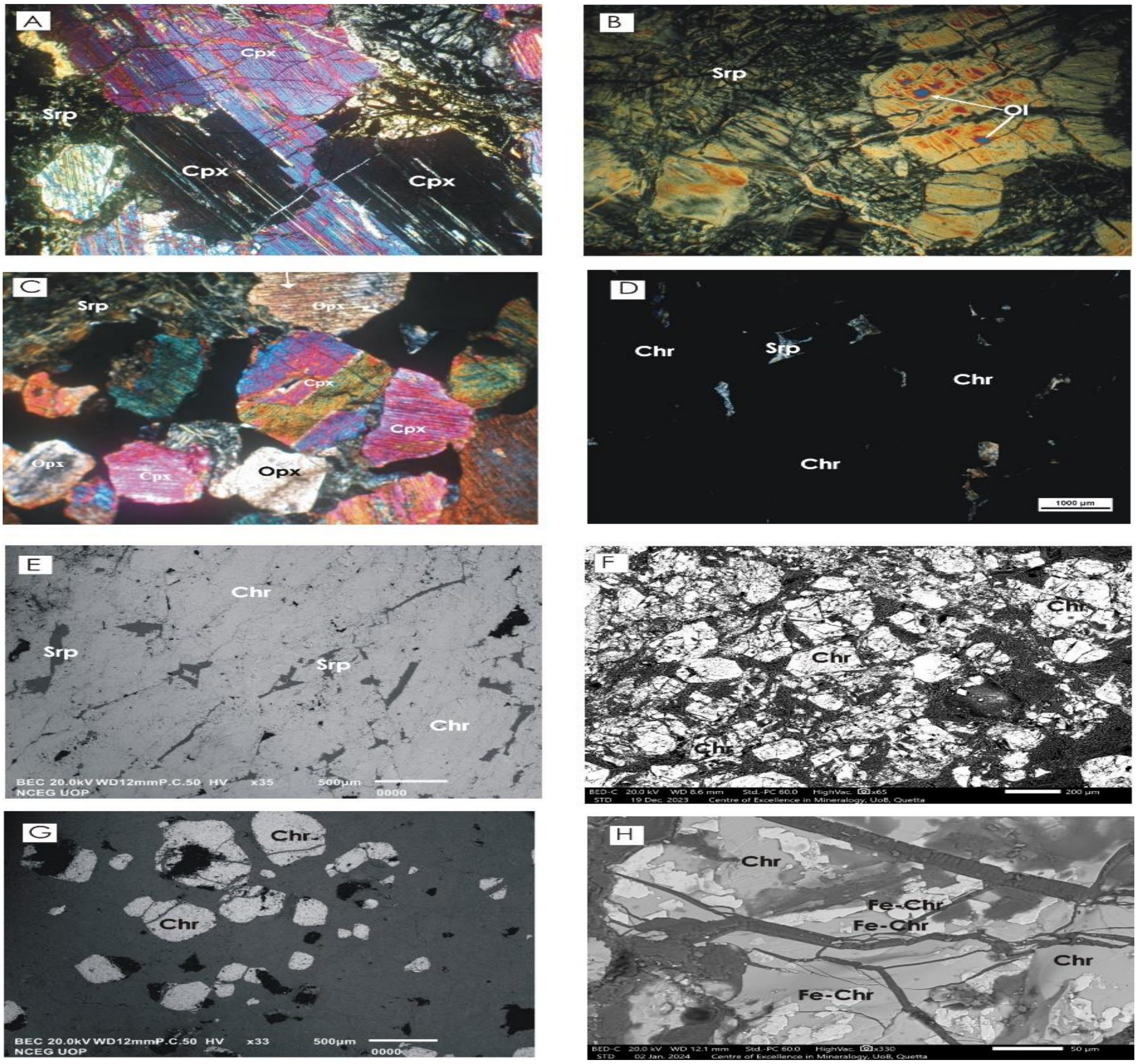


**Figure 3.** Photomicrograph (Transmitted light) of (**a**) lherzolite showing twinning and exsolution lamellae in clinopyroxene (**b**) dunite showing mesh texture formed by relict core of olivine after serpentinization (**c**) harzburgite showing subhedral grains of orthopyroxene and clinopyroxene that make hypidiomorphic granular and granobalstic textures (d) interlocking grains of chromite showing orthocumlate texture (**e**) BSE image of chromite grain showing cumulate texture (**f**) massive chromitites show brecciated texture (**g**) subhedral disseminated chromite grains (**h**) ferrit-chromite alteration. (Ol=Olivine, Srp=Serpentine Cpx=Clinopyroxene, Opx= Orthopyroxene, Chr=chromite,

## 5. METHODOLOGY

Several samples of chromitite in the mantle portion of Khanozai ophiolite were collected in the field. Polished sections were prepared of standard size for petrographic and geochemical studies of silicate and BMS inclusions in the chromitite. The selected samples were coated with a gold coater. Then these samples were analyzed for mineral chemistry of silicate and BMS inclusions using SEM-EDX Model No (Jeol JSM-IT200) with voltage of (20 Kev). These analysis SEM Laboratory of the Centre of Excellence in Mineralogy, University of Balochistan, Quetta, Pakistan.

## 6. RESULTS

### 6.1. Silicate inclusions

Unaltered chromite grains host several inclusions of the primary silicate mineral phases such as amphibole, clinopyroxene, olivine, serpentine and chlorite (Fig. 4a–d). These inclusions are randomly distributed within chromite grains. These silicate mineral inclusions range from 10μm to 30μm in size and are subhedral to euhedral in shape. Amphibole is the most common inclusion ranging in size up to 25 μm and make subhedral shapes (Fig.4a). The major oxide composition of amphibole inclusions contains 51.2-53.2 wt.% $SiO_2$, 20.1-21.6 wt.% MgO, 8.1-10.4 wt.% $Al_2O_3$, 1.1-2.2 wt.% $Na_2O$ and 10.9-12.1 wt.% CaO. The contents of $SiO_2$, MgO, FeO, and CaO in Clinopyroxene ranges from 54.1-55.5 wt.%, 16.2-17.5 wt.%, 1.2-2.1 wt.%, and 24.5-25.2 wt.%, respectively. Composition of olivine ranges from 42.1-43.3 wt.% $SiO_2$, 2.4-3.1 wt.% FeO and 50.8-52.1 wt.% MgO. Sizes of clinopyroxene and olivine reaches up to 20 and 25 μm, respectively (Fig.4b-d; Table. 1).

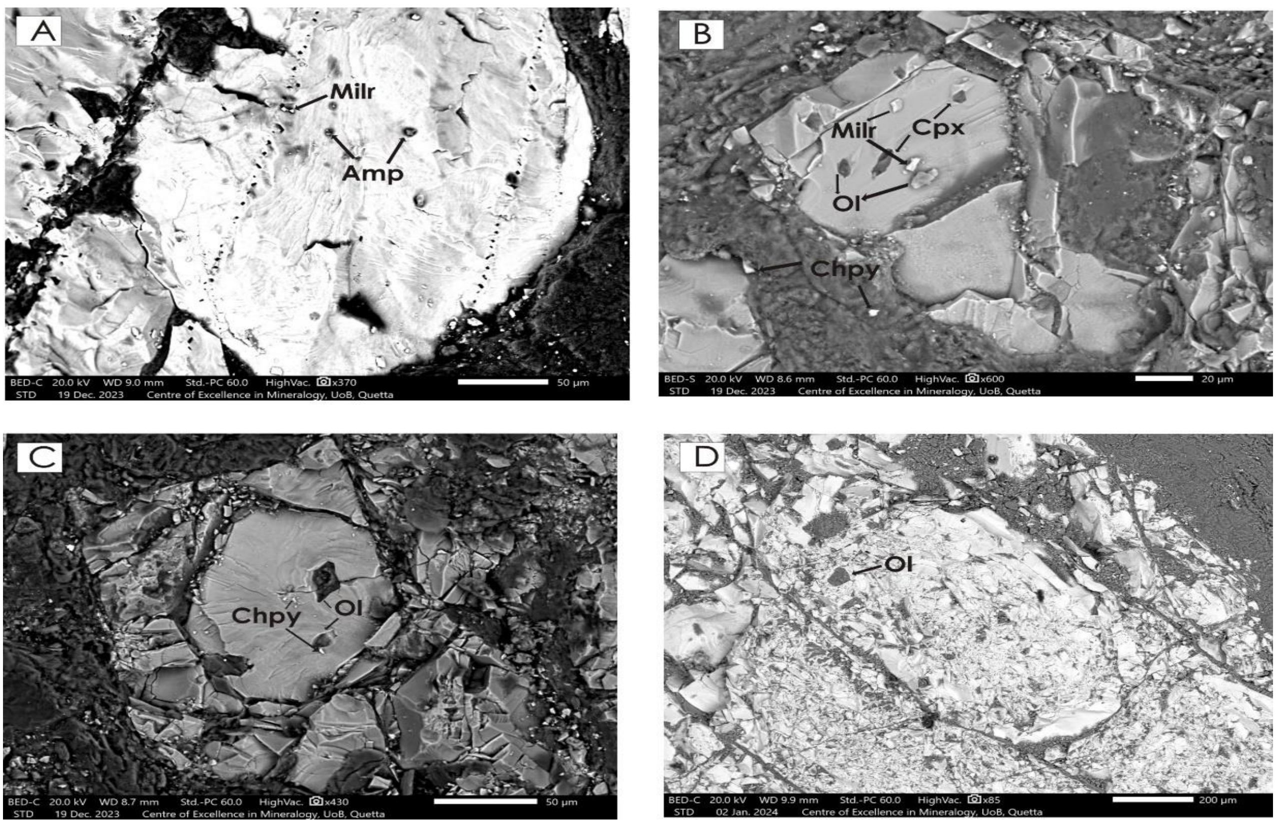


**Figure 4**. BSE image shows (**a**) amphibole and millerite inclusions (**b**) clinopyroxene, olivine, millerite, and chalcopyrite inclusions (**c**) olivine and chalcopyrite inclusions (**d**) altered olivine inclusion. These all inclusions

occur within chromite grains except chalcopyrite in fig. (b) which occurs in serpentinized matrix in the fractures. Amp=amphibole, ol=olivine, cpx=clinopyroxene, milr=millerite, and chpy=chalcopyrite.

**Table. 1.** Representative SEM composition of silicate inclusion in Khanozai chromitite; amp= amphibole, Cpx=Clinopyroxene, Ol=Olivine, bdl= below detection limit.

| Sample # | Ch-1 | Ch-2 | Ch-25 | Ch-26 | Ch-14 | Ch-14b | Ch-25 | Ch-3 | Ch-14 | Ch-25 | Ch-26 |
|---|---|---|---|---|---|---|---|---|---|---|---|
| inclusions # | 2 | 3 | 1 | 3 | 2 | 2 | 1 | 1 | 3 | 2 | 1 |
| Mineral | Amp | Amp | Amp | Amp | Cpx | Cpx | Cpx | Ol | Ol | Ol | Ol |
| SiO2 | 51.2 | 53.1 | 53.2 | 52.6 | 55.5 | 54.7 | 54.1 | 42.1 | 43.3 | 42.5 | 42.1 |
| FeO | 2.1 | 1.2 | 1.4 | 1.9 | 1.2 | 1.6 | 1.3 | 2.4 | 4.1 | 3.7 | 2.8 |
| MgO | 20.5 | 20.1 | 21.3 | 21.6 | 16.2 | 17.1 | 17.5 | 51.7 | 50.8 | 52.1 | 51.8 |
| Al2O3 | 9.7 | 10.4 | 8.1 | 8.8 | 1.5 | 0.5 | 0.9 | bdl | bdl | bdl | bdl |
| 2O3 | 1.1 | 2.3 | 2.1 | 0.9 | 0.12 | 0.4 | 0.7 | 1.7 | 0.9 | 0.8 | 0.9 |
| CaO | 12.1 | 11.6 | 11.1 | 10.9 | 24.5 | 25.2 | 24.8 | bdl | bdl | bdl | bdl |
| Na2O | 1.3 | 1.1 | 1.9 | 2.2 | bdl | bdl | bdl | 0.6 | 0.4 | 0.6 | 0.5 |
| Total | 98 | 99.8 | 99.1 | 98.9 | 99.02 | 99.5 | 99.3 | 98.5 | 99.5 | 99.7 | 98.1 |

## 6.2. Base metal sulfides (BMS)

Primary inclusions of base metal sulfide (BMS) minerals found in Khanozai chromitite are usually subhedral in shape and range in size from less than 10 µm to 30 µm in size. The BMS inclusions occur either as monophase or composite grains associated with silicates, chromite and/or other BMS (Fig. 4 and 5). BMS inclusions include millerite, chalcopyrite, stibnite, and barium sulfide phases. Millerite, subhedral in shape and less than 10 µm in size, is the frequently occurring BMS inclusion found as a primary inclusion (Fig. 5a). This reveals that millerite is a common magmatic sulfide phase. The second most abundant BMS inclusion is chalcopyrite found in Khanozai chromitite (Fig. 5 b and c). Chalcopyrite is subhedral to anhedral in shape and reaches up to 30 µm in size. The occurrence of chalcopyrite indicates hydrothermal activities during chromitite formation. Less common stibnite, linnaeite and pyrite are also observed (Fig. 5 d, e, and f). All these inclusions are found within chromite grains, and some are present in the cracks of chromite grains. Millerites composition contain Ni, Fe and S contents range between 58.9-61.2, 3.1-5.4 and 34.1-36.1 wt.%, respectively. The chalcopyrite grains contain Fe (27.4-28.3 wt.%), S (38-39.1 wt.%) and Cu (31.2-32.5 wt.%). Similarly, stibnite is composed of 1.1-1.2 wt.% Fe, 25.7-26.1 wt.%, and 69.3-68.7 wt.% S (Table 2).

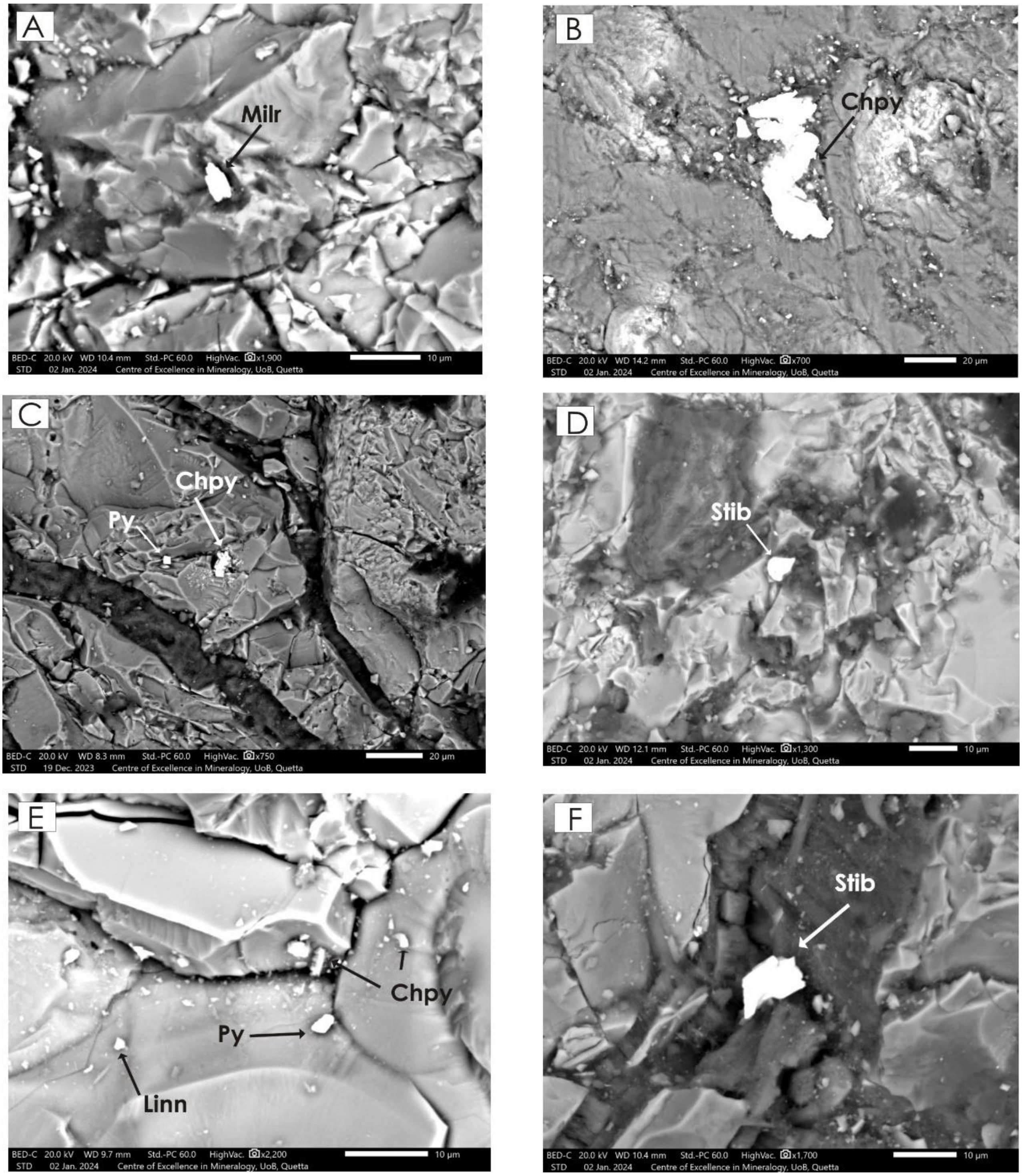


**Figure 5**. BSE image shows (**a**) subhedral millerite inclusions (**b**) a large and several small, disseminated chalcopyrite inclusions (**c**) inclusions of chalcopyrite and euhedral pyrite (**d**) stibnite inclusion (e) small, dispersed inclusions of chalcopyrite, pyrite, and linnaeite (**f**) a large, isolated inclusions of stibnite. These all inclusions occur within chromite grains except stibnite in fig. (f) which occurs in serpentinized matrix in the fractures of chromite grain. Milr=millerite, chpy=chalcopyrite, py=pyrite, stib=stibnite and linn=linnaeite

**Table. 2.** Representative SEM composition of BMS inclusion in Khanozai chromitite; Milr=millerite, Chpy=chalcopyrite, Stib=stibnite, Linn=Linnaeite, bdl= below detection limit

| Sample # | Ch-1 | Ch-2 | Ch-14 | Ch-25 | Ch-3 | Ch-14 | Ch-25 | Ch-26 | Ch-25 | Ch-14b | Ch-26 |
|---|---|---|---|---|---|---|---|---|---|---|---|
| Inclusion # | 1 | 2 | 1 | 3 | 2 | 2 | 2 | 1 | 1 | 1 | 1 |
| Mineral | Milr | Milr | Milr | Milr | Chpy | Chpy | Chpy | Stib | Stib | Linn | Py |
| Ni | 59.1 | 60.4 | 58.9 | 61.2 | 0.5 | 0.3 | 0.6 | bdl | bdl | 13.1 | 0.4 |
| Fe | 3.6 | 3.1 | 5.4 | 4.1 | 27.4 | 28.3 | 27.5 | 1.1 | 1.2 | 9 | 46.1 |
| S | 34.2 | 36.1 | 34.3 | 34.1 | 38 | 39.1 | 38.3 | 26.1 | 25.7 | 24 | 53.2 |
| Cu | 0.7 | bdl | bdl | bdl | 32.1 | 31.2 | 32.5 | 1.4 | 1.6 | bdl | bdl |
| As | 0.4 | bdl | bdl | bdl | 0.4 | 0.9 | 0.7 | 1.5 | 2.2 | bdl | bdl |
| Co | bdl | bdl | bdl | bdl | bdl | bdl | bdl | bdl | bdl | 51.5 | bdl |
| Sb | bdl | bdl | bdl | bdl | bdl | bdl | bdl | 69.3 | 68.7 | 0.9 | bdl |
| Total | 98 | 99.6 | 98.6 | 99.4 | 98.4 | 99.8 | 99.6 | 99.4 | 99.4 | 98.5 | 99.7 |

## 7. DISCUSSION

Inclusions of silicate and base metal sulfide (BMS) minerals in chromite have been described from several ophiolitic chromitites, such as Kempirsai ophiolite (4), Oman ophiolite (18-19), Sartohay ophiolite (10), Muğla ophiolite (21), Moa-Mayari and Zambales ophiolites (22). These inclusions are mainly hydrous silicates (amphibole), anhydrous silicates (olivine, pyroxene), base-metal sulfides are common in these ophiolitic chromitites.

Various kinds of minerals inclusions are found in the Chromite of Khanozai ophiolite. The shapes of these inclusions tend to follow the growth plane of host chromite. The Khanozai chromitite contains inclusions of several types of hydrous silicates, anhydrous silicates and BMS minerals. Hydrous silicate inclusions are mainly amphibole, while olivine and clinopyroxene are the most common anhydrous silicates inclusions and base-metal sulfides inclusions are mainly millerite, chalcopyrite, stibnite, and rarely pyrite and linnaeite. Like other Al-rich chromitite, no specific PGM and alloy are found, although we carried out a detailed mineralogical investigation.

Researchers have been proposed two mechanisms for the formation of silicate inclusions in chromite: 1) entrapment during chromite crystallization in magmas, 2) entrapment at the transition from magmatic to hydrothermal conditions during recrystallization of chromite (23). However, some authors believe that only single (unassociated) silicate inclusions are formed by entrapment of crystals, while multiple-phases inclusions formed due to entrapment of crystals and volatile rich melt during chromite crystallization (18). Silicate minerals may be enclosed during post-magmatic recrystallization of chromite may enclosed the silicate inclusions because of the sintering (24). Mineralogical and textural characteristics of silicate inclusion found in Khanozai chromitite suggest magmatic origin for some inclusions, however, the majority probably formed during sub-solidus recrystallization of chromite. The monomineralic inclusions of olivine and clinopyroxene display largely subhedral with rare euhedral shapes, reveals that these inclusions were trapped and crystallized as solitary crystals before chromite. In contrast, anhydrous silicate such as amphibole exhibit anhedral shapes and mostly occur composite, may be formed by complicated reactions between crystals and melts (25). According to (26) findings, chemical reaction, at pressures <10 kbar, between chromite, clinopyroxene and melt can form amphibole. The formation of amphibole can also be result by the reaction of orthopyroxene with volatile-rich melt. Earlier work on the origin of base-metal sulfide inclusions (4,18, 23, 27) have proposed two models: 1) sulfidation reactions between silicates and a sulfide-bearing fluid, and 2) separation of silicate magma from an immiscible sulfide liquid. Sulfides in chromite are considered commonly as primary phase, and euhedral grains of sulfide minerals are believed to originate before the host chromite (4). BMS inclusions in our samples occur monophase sulfide as well as silicate-sulfide polyphase inclusions in chromite grains (Figs.3 and 4). Therefore, we suggest that the BMS inclusion in Khanozai chromitite formed from the separation of an immiscible sulfide liquid from mafic magma. The separation of immiscible sulfide liquids from mafic magma can occur during precipitation of chromite (28), and usually, these sulfide liquids contain some Cu contents (29). The formation of isolated Cu sulfides (chalcopyrite) inclusions in chromite of Khanozai ophiolite proved the mechanism separation of silicate magma from an immiscible sulfide liquid for the origin of these BMS inclusions. Chromite recrystallizes at low temperatures (500°C to 600°C) (30), and can trap a wide range of, melt, fluid, and minerals inclusions near to chromite. During late stage melt evolution the exsolved fluids tend to wet efficiently the chromite surfaces than silicate surfaces, and sulfide rich melts show the same behavior (31).

## CONCLUSION

Khanozai ophiolite is the part of Zhob valley ophiolites stretches from Zhob town to Quetta around 300 km in western Pakistan. Khanozai ophiolite contains wide peridotite which contains several chromitite bodies. Chromite from these bodies contains several kinds of mineral inclusions. They are dominated by silicate inclusions like amphibole, olivine and clinopyroxene with base metal sulfides inclusions such as millerite, chalcopyrite, stibnite, and barium sulfide phases. These inclusions are found as monophase as well as multi-phases inclusions. Olivine and clinopyroxene occur as monomineralic inclusions and exhibit subhedral granular with occasional euhedral shape, indicate that these inclusions formed before the chromite grains and were trapped as isolated crystals. While amphibole forms anhedral shapes and usually found in association with clinopyroxene, may formed during the recrystallization of chromite by reactions of crystallized minerals with melts. BMS inclusions formed as isolated crystals or silicate-sulfide minerals and they are formed due to separation of silicate magma from an immiscible sulfide liquid.

## Acknowledgement

Authors are thankful to Fawad Ali Khan Achakzai (SEM Lab operator) who has helped us in lab analysis and Hikmat Ullah Kakar for the provision of the chromitite samples.

## DECLARATIONS

**Funding**: No funding is availed for this study.

**Conflicts of interest/Competing interests**: The authors declare no conflict of interest or competing interests.

**Authors' contributions:**

All the authors have equally contributed to this study from conceptualization to the write up of the final draft.

## REFERENCES

[1] Cai. K, Sun. M, Yuan. C, Zhao. G, Xiao. W, Long. X, Keketuohai mafic–ultramafic complex in the Chinese Altai, NW China: petrogenesis and geodynamic significance. Chemical Geology, (2012) 294– 295, 26–41.

[2] Ghosh. B, Ray. J, Morishita. T, Grain-scale plastic deformation of chromite from podiform chromitite of the Naga-Manipur ophiolite belt, India: Implication to mantle dynamics, Ore Geology Reviews, 56 (2014) 199–208.

[3] Maurel. C, Maurel. P, Etude experimental de la soulbilitè du chrome dans les basin silicates basiques et sa distribution entre liquide et mineraux coexistants: conditions d'existence du spinelle chromifere, Bulletin de Mineralogie, 105 (1982) 197–202.

[4] Melcher. F, Grum. W, Simon. G, Thalhammer. T.V, Stumpfl. E.F, Petrogenesis of the Ophiolitic Giant Chromite Deposits of Kempirsai, Kazakhstan: a Study of Solid and Fluid Inclusions in Chromite. Journal of Petrology, 38(10) (1997) 1419–1458.

[5] Kamenetsky. V.S, Crawford. A.J, Meffre. S, Factors controlling chemistry of magmatic spinel: an empirical study of associated olivine, Cr-spinel and melt inclusions from primitive rocks. Journal of Petrology, 42(4) (2001) 655–671.

[6] Arai. S, Okamura. H, Kadoshima. K, Tanaka. C, Suzuki. K, Ishimaru. S, Chemical characteristics of chromian spinel in plutonic rocks: implications for deep magma processes and discrimination of tectonic setting, Island Arc, 20 (2011) 125–137.

[7] Zaccarini. F, Garuti. G, Proenza. J.A, Campos. L, Thalhammer. O.A.R, Aiglsperger. T, Lewis. J, Chromite and platinum-group-elements mineralization in the Santa Elena ophiolitic ultramafic nappe (Costa Rica): geodynamic implications, Geologica Acta, 9(3) (2011) 407–423.

[8] Ulhaq. E, Petrology of Mantle Rocks from the Khanozai Ophiolites, Northern Balochistan, Pakistan. [M.Phil Thesis, University of Balochistan], (2018) 70.

[9] Khan. M.A, Ulrich. T, Kakar. M.I, Akmaz. R.M, Siddiqui. R.H, Ali. L, Genesis and geotectonic setting of podiform chromitites from the Zhob Valley Ophiolite, Pakistan: inferences from chromite composition. Eposides 43(4) (2020) 1017–1039.

[10] Khan. M, Kerr. A.C, Mahmood. K, Formation and tectonic evolution of the Cretaceous-Jurassic Muslim Bagh ophiolitic complex, Pakistan: implications for the composite tectonic setting of

ophiolites. Journal of Asian Earth Sciences 31(2007) 112–127.

[11] Mahmood. K. Boudier. F, Gnos. E, Monié. P, Nicolas. A, 40Ar/39Ar dating of the emplacement of the Muslim Bagh ophiolite, Pakistan. Tectonophysics 250 (1995) 169–181.

[12] Jalil, R; Alard, O; Schaefer, B; Ali, L; Sajid, M; Khedr, M.Z; Shah, M.T; Anjum, M.N. Geochemistry of Waziristan Ophiolite Complex, Pakistan: Implications for Petrogenesis and Tectonic Setting. Minerals, 13(2023) 311. https://doi.org/10.3390/ min13030311

[13] Kazmi. A. H, Jan. M.Q, Geology and Tectonics of Pakistan. Graphic Publishers 55C, 6/10 Nazimabad, Karachi-Pakistan (1997) 554.

[14] Allemann. F, Time of emplacement of the Zhob Valley Ophiolite and Bela Ophiolite, Balochistan (preliminary report). In: Farah. A, Dejong, K.A., (Eds.), Geodynamics of Pakistan, Geological Survey of Pakistan, Quetta, (1979) 213-242.

[15] Kasi. A.K, Kassi. A. M, Umar. M, Manan. R.A, Kakar. M.I, Revised Lithostratigraphy and tectonic zones of the Pishin Belt, northwestern Pakistan. Journal of Himalayan Earth Sciences, 45 (2012) 60.

[16] Popal. A, Kakar. M.I, Bilqees. R, Khan. M, Ker. A.C, Geology and Petrography of Gabbroic Rocks from Khanozai Ophiolite, Northwestern Pakistan. International Research Journal of Earth Sciences, 7 (2018) 10-22.

[17] Ali. N, Petrology of Volcanic Rocks beneath the Khanozai Ophiolite, northern Balochistan, Pakistan. Unpublished M.Phil. Thesis, Centre of Excellence in Mineralogy, University of Balochistan, Pakistan, (2018) 65.

[18] Lorand. J.P, Ceuleneer. G, Silicate and base-metal sulfide inclusions in chromites from the Maqsad area (Oman ophiolite, Gulf of Oman): A model for entrapment, Lithos, 22 (1989) 173–190.

[19] Miura. M, Arai. S, Ahmed. A.H, Mizukami. T, Okuno. M, Yamamoto. S, Podiform chromitite classification revisited: A comparison of discordant and concordant chromitite pods from Wadi Hilti, northern Oman ophiolite. Journal of Asian Earth Sciences, 59 (2012) 52–61.

[20] Yazhou. T, Jingsui. Y, Tian Yazhou and Yang Jingsui, 2016. Study on the mineral inclusions in Sartohay chromitites. Acta Geologica Sinica, 90 (11) (2016) 3114–3128 (in Chinese with English abstract)

[21] Uysal. İ, Tarkian. M, Sadiklar. M.B, Zaccarini. F, Meisel. T, Garuti. G, Heidrich. S, Petrology of Al- and Crrich ophiolitic chromitites from the Muğla, SW Turkey: implications from composition of chromite, solid inclusions of platinum-group mineral, silicate, and base-metal mineral, and Os-isotope geochemistry, Contributions to Mineralogy and Petrology, 158(5) (2009) 659–674.

[22] Zhou. M.F, Robinson. P.T, Su. B.X, Gao. J.F, Li. J.W, Yang. J.S, Malpas. J, Compositions of chromite, associated minerals, and parental magmas of podiform chromite deposits: The role of slab contamination of asthenospheric melts in suprasubduction zone environments, Gondwana Research, 26(1) (2014) 262–283.

[23] McElduff. B, Stumpfl. E.F, The chromite deposits of the Troodos Complex, Cyprus-evidence for the role of a fluid phase accompanying chromite formation, Mineralium Deposita, 26(4) (1991) 307–318.

[24] Lorand. J.P, Cottin. J.Y, Na-Ti-Zr-H2O-rich mineral inclusions indicating postcumulus chrome-spinel dissolution and recrystallization in the Western Laouni mafic intrusion, Algeria, Contributions to Mineralogy and Petrology, 97(2) (1987) 251–263.

[25] Borisova. A.Y, Ceuleneer. G, Kamenetsky. V.S, Arai. S, Bejina. F, Abily. B, Bindeman. I.N, Polve. M, Parseval. P.D, Aigouy. T, Pokrovski. G.S, A new view on the petrogenesis of the Oman ophiolite chromitites from microanalyses of chromite-hosted inclusions, Journal of Petrology, 53(12) (2012) 2411–2440.

[26] Wallace. M.E, Green. D.H, The effect of bulk composition on the stability of amphibole in the upper mantle: implications for solidus positions and mantle metasomatism, Mineralogy and Petrology, 44(1–2) (1991) 1–19.

[27] Ahmed. A.H, Arai. S, Platinum-group minerals in podiform chromitites of the Oman ophiolite, The Canadian Mineralogist, 41(3) (2003) 597–616.

[28] Naldrett. A.J, Kinnaird. L, Wilson. A, Yudovskaya. M, McQuade. S, Chunnett. G, Stanley. C, Chromite composition and PGE content of Bushveld chromitites: Part 1-the lower and middle Groups. Applied Earth Science: IMM Transactions section B, 118(3–4) (2009) 131–161.

[29] Rajamani. V, Naldrett. A.J, Partitioning of Fe, Co, Ni and Cu between sulfide liquid and basaltic melts and the composition of Ni-Cu sulfide deposits, Economic Geology, 73(1) (1978) 82–93.

[30] Ballhaus. C, Berry. R.F, Green. D.H, High pressure experiment calibration of the olivine-orthopyroxene-spinel oxygen barometer: Implications for the oxidation state of the mantle, Contributions to Mineralogy and Petrology, 107(1) (1991) 27–40.

[31] Matveev. S, Ballhaus. C, Role of water in the origin of podiform chromitite deposits, Earth and Planetary Science Letters, 203(1) (2002) 235–243.

Received: 20 February 2024. Revised/Accepted: 20 March 2024.